PHYSICAL REVIEW D **88,** 036004 (2013)

Investigation of the semileptonic transition of the B into the orbitally excited charmed tensor meson

K. Azizi,[1,*] H. Sundu,[2,†] and S. Şahin[2,‡]

[1]*Department of Physics, Doğuş University, Acıbadem-Kadıköy, 34722 Istanbul, Turkey*
[2]*Department of Physics, Kocaeli University, 41380 Izmit, Turkey*

(Received 6 May 2013; revised manuscript received 18 July 2013; published 9 August 2013)

The transition form factors of the semileptonic $B \to D_2^*(2460)\ell\bar{\nu}(\ell = \tau, \mu, e)$ decay channel are calculated within the framework of the three-point QCD sum rules. The fit functions of the form factors are then used to estimate the total decay width and branching ratio of this transition. The order of branching ratio shows that this channel can be detected at the LHCb.

DOI: 10.1103/PhysRevD.88.036004 PACS numbers: 11.55.Hx, 13.20.He, 14.40.Lb

I. INTRODUCTION

As it is well known, the semileptonic decays of the B meson are very promising tools in constraining the standard model parameters, the determination of the elements of the Cabibbo-Kobayashi-Maskawa matrix, understanding the origin of the CP violation, and looking for new physics effects. Over the last few years, the radially excited charmed mesons have been the focus of much attention, both theoretically and experimentally. In 2010, the *BABAR* Collaboration reported their isolation of a number of orbitally excited charmed mesons [1]. This report has stimulated the theoretical works devoted to the semileptonic decays of the B meson into the orbitally excited charmed meson (for instance, see Refs. [2–5] and references therein). As the decays of the B meson into orbitally excited charmed mesons can provide a substantial contribution to the total semileptonic decay width, such processes deserve more detailed studies. Moreover, a better knowledge on these transitions can help us in the analysis of signals and backgrounds of inclusive and exclusive decays of b hadrons.

In this article, we calculate the transition form factors of the semileptonic decays of $B \to D_2^*(2460)\ell\bar{\nu}$ in the framework of the three-point QCD sum rules. This approach is one of the attractive and applicable nonperturbative tools to hadron physics based on the QCD Lagrangian [6]. As the $D_2^*(2460)$ is a tensor meson containing derivatives in its interpolating current, we start our calculations in the coordinate space, and then we apply the Fourier transformation to go to the momentum space. Based on the general philosophy of the method, to suppress the contributions of the higher states and continuum, we finally apply the Borel transformation and continuum subtraction, which bring some auxiliary parameters for which the working regions are determined demanding some criteria. The transition form factors are then used to calculate the decay width and branching ratio of the semileptonic decay channel under consideration.

The *BABAR* Collaboration has recently measured the ratios for the branching fractions of the B to charmed pseudoscalar D and vector D^* mesons at the τ channel to those of the e and μ channels [7]. The obtained results deviate at the level of 3.4σ from the existing theoretical predictions in the standard model [7,8]. Hence, there is a possibility that the semileptonic transitions containing heavy b and c quarks and the τ lepton bring out the effects of particles with large couplings to the heavier fermions [9]. The determination of these ratios of the branching fractions in B to the charmed tensor D_2^* channel can also be important from this point of view whether these anomalies in the pseudoscalar and vector channels exist in the tensor channel or not. We will be able to answer this question when having the experimental data in this channel. By the aforementioned experimental progress on the identification and spectroscopy of the orbitally excited charmed mesons as well as the developments at the LHC and by considering the orders of the branching ratios in the tensor channel, we hope it will be possible in the near future.

This article is arranged as follows. We derive the QCD sum rules for the form factors, defining the semileptonic $B \to D_2^*(2460)\ell\bar{\nu}$ transition in Sec. II. The last section is devoted to the numerical analysis of the form factors, calculations of the branching ratios of the transition under consideration at different lepton channels, and our concluding remarks.

II. QCD SUM RULES FOR TRANSITION FORM FACTORS OF $B \to D_2^*(2460)\ell\bar{\nu}$

This section is dedicated to the calculation of the form factors of the $B \to D_2^*(2460)\ell\bar{\nu}$ transition applying the QCD sum rules technique. The starting point is to consider the following tree-point correlation function:

$$\Pi_{\mu\alpha\beta}(q^2) = i^2 \int d^4x \int d^4y e^{-ip.x} e^{ip'.y} \times \langle 0 \mid \mathcal{T}[J^{D_2^*}_{\alpha\beta}(y) J^{\mathrm{tr}}_{\mu}(0) J^{B^\dagger}(x)] \mid 0 \rangle, \quad (1)$$

*kazizi@dogus.edu.tr
†hayriye.sundu@kocaeli.edu.tr
‡095131004@kocaeli.edu.tr

where $\mathcal{T}$ is the time-ordering operator and $J_\mu^{\rm tr}(0) = \bar{c}(0)\gamma_\mu(1-\gamma_5)b(0)$ is the transition current. Also, the interpolating currents of the B and $D_2^*(2460)$ mesons are written in terms of the quark fields as

$$J^B(x) = \bar{u}(x)\gamma_5 b(x) \tag{2}$$

$$J^{D_2^*}_{\alpha\beta}(y) = \frac{i}{2}[\bar{u}(y)\gamma_\alpha \overleftrightarrow{\mathcal{D}}_\beta(y)c(y) + \bar{u}(y)\gamma_\beta \overleftrightarrow{\mathcal{D}}_\alpha(y)c(y)], \tag{3}$$

where the $\overleftrightarrow{\mathcal{D}}_\beta(y)$ denotes the four-derivative with respect to y acting on the left and right, simultaneously, and is given as

$$\overleftrightarrow{\mathcal{D}}_\beta(y) = \frac{1}{2}[\vec{\mathcal{D}}_\beta(y) - \overleftarrow{\mathcal{D}}_\beta(y)], \tag{4}$$

with

$$\begin{aligned}\vec{\mathcal{D}}_\beta(y) &= \vec{\partial}_\beta(y) - i\frac{g}{2}\lambda^a A^a_\beta(y),\\ \overleftarrow{\mathcal{D}}_\beta(y) &= \overleftarrow{\partial}_\beta(y) + i\frac{g}{2}\lambda^a A^a_\beta(y),\end{aligned} \tag{5}$$

where λ^a are the Gell-Mann matrices and $A^a_\beta(x)$ is the external gluon fields. These fields are expressed in terms of the gluon field strength tensor, using the Fock-Schwinger gauge ($x^\beta A^a_\beta(y) = 0$),

$$\begin{aligned}A^a_\beta(y) &= \int_0^1 d\alpha\alpha y_\nu G^a_{\nu\beta}(\alpha y)\\ &= \frac{1}{2}y_\nu G^a_{\nu\beta}(0) + \frac{1}{3}y_\eta y_\nu \mathcal{D}_\eta G^a_{\nu\beta}(0) + \cdots.\end{aligned} \tag{6}$$

Following the general idea of the QCD sum rule approach, the aforementioned correlation function is calculated via two different ways: once in terms of hadronic degrees of freedom, called the phenomenological or physical side, and the other in terms of QCD degrees of freedom, called the theoretical or QCD side. By matching these two representations, the QCD sum rules for the form factors are obtained. To stamp down the contributions of the higher states and continuum, we will apply a double Borel transformation with respect to the momentum squared of the initial and final states and will use the quark-hadron duality assumption.

A. Phenomenological side

On the phenomenological side, the correlation function is obtained inserting two complete sets of intermediate states with the same quantum numbers as the interpolating currents J^B and $J^{D_2^*}$ into Eq. (1). After performing four-integrals over x and y, we get

$$\Pi^{\rm phen}_{\mu\alpha\beta}(q^2) = \frac{\langle 0 \mid J^{D_2^*}_{\alpha\beta}(0) \mid D_2^*(p',\epsilon)\rangle\langle D_2^*(p',\epsilon) \mid J^{\rm tr}_\mu(0) \mid B(p)\rangle\langle B(p) \mid J^\dagger_B(0) \mid 0\rangle}{(p^2 - m_B^2)(p'^2 - m^2_{D_2^*(2460)})} + \cdots, \tag{7}$$

where $\cdots$ represents contributions of the higher states and continuum and ϵ is the polarization tensor of the $D_2^*(2460)$ tensor meson. To proceed, we need to define the following matrix elements in terms of decay constants and form factors:

$$\begin{aligned}\langle 0 \mid J^{D_2^*}_{\alpha\beta}(0) \mid D_2^*(p',\epsilon)\rangle &= m^3_{D_2^*} f_{D_2^*}\epsilon_{\alpha\beta}\\ \langle B(p) \mid J^\dagger_B(0) \mid 0\rangle &= -i\frac{f_B m_B^2}{m_u + m_b}\\ \langle D_2^*(p',\epsilon) \mid J^{\rm tr}_\mu(0) \mid B(p)\rangle &= h(q^2)\varepsilon_{\mu\nu\lambda\eta}\epsilon^{*\nu\theta}P_\theta P^\lambda q_\eta - iK(q^2)\epsilon^*_{\mu\nu}P^\nu\\ &\quad - i\epsilon^*_{\lambda\eta}P^\lambda P^\eta[P_\mu b_+(q^2) + q_\mu b_-(q^2)],\end{aligned} \tag{8}$$

where $h(q^2)$, $K(q^2)$, $b_+(q^2)$, and $b_-(q^2)$ are transition form factors, and $f_{D_2^*}$ and f_B are leptonic decay constants of D_2^* and B mesons, respectively. By combining Eqs. (7) and (8) and performing a summation over the polarization tensors using

$$\epsilon_{\alpha\beta}\epsilon^*_{\nu\theta} = \frac{1}{2}T_{\alpha\nu}T_{\beta\theta} + \frac{1}{2}T_{\alpha\theta}T_{\beta\nu} - \frac{1}{3}T_{\alpha\beta}T_{\nu\theta}, \tag{9}$$

with

$$T_{\alpha\nu} = -g_{\alpha\nu} + \frac{p'_\alpha p'_\nu}{m^2_{D_2^*(2460)}}, \tag{10}$$

the final representation of the physical side is obtained as

$$\begin{aligned}\Pi^{\rm phen}_{\mu\alpha\beta} &= \frac{f_{D_2^*}f_B m_{D_2^*}m_B^2}{8(m_b+m_u)(p^2-m_B^2)(p'^2-m^2_{D_2^*})}\\ &\times\Big\{\frac{2}{3}[-\Delta K(q^2) + \Delta' b_-(q^2)]q_\mu g_{\beta\alpha}\\ &+ \frac{2}{3}[(\Delta - 4m^2_{D_2^*})K(q^2) + \Delta' b_+(q^2)]P_\mu g_{\beta\alpha}\\ &+ i(\Delta - 4m^2_{D_2^*})h(q^2)\varepsilon_{\lambda\nu\beta\mu}P_\lambda P_\alpha q_\nu\\ &+ \Delta K(q^2)q_\alpha g_{\beta\mu} + \text{other structures}\Big\} + \cdots,\end{aligned} \tag{11}$$

where

$$\Delta = m_B^2 + 3m_{D_2^*(2460)}^2 - q^2,$$
$$\Delta' = m_B^4 - 2m_B^2(m_{D_2^*(2460)}^2 + q^2) + (m_{D_2^*(2460)}^2 - q^2)^2. \quad (12)$$

We will use the explicitly written structures to find the aforementioned form factors.

B. QCD side

On the QCD side, the correlation function is calculated by expanding the time-ordering product of the B and $D_2^*(2460)$ mesons' currents and the transition current via operator product expansion (OPE) in the deep Euclidean region in which the short- (perturbative) and long-distance (nonperturbative) contributions are separated. By inserting the previously represented currents into Eq. (1) and after contracting out all quark fields applying the Wick's theorem, we obtain

$$\Pi^{\rm QCD}_{\mu\alpha\beta}(q^2) = \frac{-i^3}{4}\int d^4x\int d^4y e^{-ip\cdot x}e^{ip'\cdot y} \times \{{\rm Tr}[S_u^{ik}(x-y)\gamma_\alpha \overleftrightarrow{\mathcal{D}}_\beta(y) S_c^{ij}(y)\gamma_\mu(1-\gamma_5) \times S_b(-x)^{jk}\gamma_5] + [\beta \leftrightarrow \alpha]\}. \quad (13)$$

To proceed, we need the expressions of the heavy and light quarks propagators. Up to the terms considered in this study, they are, respectively, given as

$$S_Q^{ij}(x) = \frac{i}{(2\pi)^4}\int d^4k e^{-ik\cdot x}\left\{\frac{\not k + m_c}{k^2 - m_c^2}\delta_{ij} + \cdots\right\}, \quad (14)$$

and

$$S_q^{ij}(x) = i\frac{\not x}{2\pi^2x^4}\delta_{ij} - \frac{m_q}{4\pi^2x^2}\delta_{ij} - \frac{\langle\bar qq\rangle}{12}\left(1 - i\frac{m_q}{4}\not x\right)\delta_{ij} - \frac{x^2}{192}m_0^2\langle\bar qq\rangle\left(1 - i\frac{m_q}{6}\not x\right)\delta_{ij} + \cdots. \quad (15)$$

After putting the expressions of the quarks propagators and applying the derivatives with respect to x and y in Eq. (13), the following expression for the QCD side of the correlation function in coordinate space is obtained:

$$\Pi^{\rm QCD}_{\mu\alpha\beta}(q^2) = \frac{i^5N_c}{4}\int\frac{d^4k}{(2\pi)^4}\int\frac{d^4k_1}{(2\pi)^4}\int d^4x e^{-ip\cdot x}\int d^4y e^{ip'\cdot y}\frac{e^{-ik\cdot y}}{(k^2-m_c^2)}\frac{e^{ik_1\cdot x}}{(k_1^2-m_b^2)}\Big\{ik_\beta\,{\rm Tr}\Big[\Big(\frac{i(\not x - \not y)}{2\pi^2(x-y)^4} - \frac{\langle\bar uu\rangle}{12} - \frac{(x-y)^2}{192}m_0^2\langle\bar uu\rangle\Big)\gamma_\alpha(\not k + m_c)\gamma_\mu(1-\gamma_5)(\not k_1 + m_b)\gamma_5\Big] + {\rm Tr}\Big[\Big(\frac{i}{2\pi^2}\Big(\frac{4(x-y)_\beta(\not x - \not y)}{(x-y)^6} - \frac{\gamma_\beta}{(x-y)^4}\Big) + \frac{(x-y)_\beta}{96}m_0^2\langle\bar uu\rangle\Big)\gamma_\alpha(\not k + m_c)\gamma_\mu(1-\gamma_5)(\not k_1 + m_b)\gamma_5\Big] + [\beta\leftrightarrow\alpha]\Big\}, \quad (16)$$

where $N_c = 3$ is the color factor. To perform the integrals, first, the terms containing $\frac{1}{((x-y)^2)^n}$ are transformed to the momentum space $[(x-y)\to t]$; then, the replacements $x_\mu \to i\frac{\partial}{\partial p_\mu}$ and $y_\mu \to -i\frac{\partial}{\partial p'_\mu}$ are made. The four-integrals over x and y give us two Dirac Delta functions, which help us perform the four-integrals over k and k_1. The last four-integral over t is performed using the Feynman parametrization and

$$\int d^4t\frac{(t^2)^\beta}{(t^2+L)^\alpha} = \frac{i\pi^2(-1)^{\beta-\alpha}\Gamma(\beta+2)\Gamma(\alpha-\beta-2)}{\Gamma(2)\Gamma(\alpha)[-L]^{\alpha-\beta-2}}. \quad (17)$$

As a result, the QCD side of the correlation function is obtained in terms of the corresponding structures as

$$\Pi^{\rm QCD}_{\mu\alpha\beta}(q^2) = (\Pi_1^{\rm pert}(q^2) + \Pi_1^{\rm nonpert}(q^2))q_\alpha g_{\beta\mu} + (\Pi_2^{\rm pert}(q^2) + \Pi_2^{\rm nonpert}(q^2))q_\mu g_{\beta\alpha} + (\Pi_3^{\rm pert}(q^2) + \Pi_3^{\rm nonpert}(q^2))P_\mu g_{\beta\alpha} + (\Pi_4^{\rm pert}(q^2) + \Pi_4^{\rm nonpert}(q^2))\varepsilon_{\lambda\nu\beta\mu}P_\lambda P_\alpha q_\nu + \text{other structures}, \quad (18)$$

where the perturbative parts $\Pi_i^{\rm pert}(q^2)$ are given in terms of double dispersion integrals as

$$\Pi_i^{\rm pert}(q^2) = \int ds\int ds'\frac{\rho_i(s,s',q^2)}{(s-p^2)(s'-p'^2)}. \quad (19)$$

The spectral densities $\rho_i(s,s',q^2)$ are given by the imaginary parts of the $\Pi_i^{\rm pert}(q^2)$ functions, i.e., $\rho_i(s,s',q^2) = \frac{1}{\pi}{\rm Im}[\Pi_i^{\rm pert}(q^2)]$. After lengthy calculations, the spectral densities corresponding to the selected structures are obtained as

$$\rho_1(s,s',q^2)=\int_0^1 dx\int_0^{1-x}dy\Big\{\frac{1}{64\pi^2(x+y-1)^3}[m_b(x+y-1)^3(8x^2-8y^2+6x-6y-6)+3m_c(8x^5+6x^4(4y-3)$$
$$-6x(y-1)^2(3+2y+4y^2)-2(2+3y+4y^2)(y-1)^3+2x^3(1-18y+8y^2)+x^2(22-5y-16y^3))]\Big\},$$
$$\rho_2(s,s',q^2)=\int_0^1 dx\int_0^{1-x}dy\Big\{\frac{-1}{32\pi^2(x+y-1)^3}[m_b(x+y-1)^3(2x^2-2y^2+6x-6y-3)$$
$$+3m_c(2x^5-3x(y-1)^2(1+2y^2)-(y-1)^3(1+2y^2)+x^3(5-12y+4y^2)$$
$$+6x^4(y-1)+x^2(1+4y-4y^3))]\Big\},$$
$$\rho_3(s,s',q^2)=\int_0^1 dx\int_0^{1-x}dy\Big\{\frac{1}{32\pi^2(x+y-1)^3}[m_b(2x^2+2y^2+x(6+4y)+6y-3)(x+y-1)^3$$
$$+3m_c(2x^5+2x^4(5y-3)+(y-1)^3(1+2y^2)+x(y-1)^2(3-4y+10y^2)+x^3(7-24y+20y^2)$$
$$+x^2(20y^3-36y^2+20y-5))]\Big\},$$
$$\rho_4(s,s',q^2)=0. \tag{20}$$

For the nonperturbative parts, we get

$$\Pi_1^{\text{nonpert}}(q^2)=\Big\{\frac{m_b^4+4m_b^2m_c^2+2m_b^2(m_c^2-q^2)+(m_c^2-q^2)^2}{64r^2r'^2}+\frac{m_b^2m_c^2(m_b^2+m_c^2-q^2)}{32r^2r'^3}$$
$$+\frac{m_b^3m_c+m_b^2m_c^2+2m_bm_c^3+m_c^4-m_c^2q^2}{32rr'^3}-\frac{m_b^2+4m_bm_c+m_c^2-q^2}{64rr'^2}$$
$$+\frac{m_b^4+2m_b^3m_c+m_b^2m_c^2-m_b^2q^2}{32r^3r'}+\frac{3m_b^2+2m_bm_c+3m_c^2-3q^2}{64r^2r'}+\frac{m_b^2}{32r^3}$$
$$+\frac{m_c^2}{32r'^3}-\frac{1}{32r'^2}+\frac{1}{32r^2}-\frac{1}{32rr'}\Big\}m_0^2\langle\bar{u}u\rangle-\Big(\frac{m_b^2+2m_bm_c+m_c^2-q^2}{16rr'}+\frac{1}{16r}+\frac{1}{16r'}\Big)\langle\bar{u}u\rangle,$$
$$\Pi_2^{\text{nonpert}}(q^2)=0,\ \Pi_3^{\text{nonpert}}(q^2)=\frac{m_0^2\langle\bar{u}u\rangle}{8rr'},$$
$$\Pi_4^{\text{nonpert}}(q^2)=-i\Big\{\frac{m_c^2}{32rr'^3}+\frac{m_b^2}{32r^3r'}+\frac{m_b^2+m_c^2-q^2}{64r^2r'^2}-\frac{1}{32r^2r'}\Big\}m_0^2\langle\bar{u}u\rangle+i\frac{\langle\bar{u}u\rangle}{16rr'}, \tag{21}$$

where $r=p^2-m_b^2$ and $r'=p'^2-m_c^2$.

To obtain sum rules for the form factors, the coefficients of the same structures from both sides of the correlation functions are matched. To suppress the contributions of the higher states and continuum, we apply a double Borel transformation with respect to the initial and final momenta squared, using

$$\hat{B}\frac{1}{(p^2-m_b^2)^m}\frac{1}{(p'^2-m_c^2)^n}\to\frac{(-1)^{m+n}}{\Gamma[m]\Gamma[n]}e^{-m_b^2/M^2}e^{-m_c^2/M'^2}\frac{1}{(M^2)^{m-1}(M'^2)^{n-1}}, \tag{22}$$

where M^2 and M'^2 are Borel mass parameters. We also use the quark-hadron duality assumption, i.e.,

$$\rho^{\text{higher states}}(s,s',q^2)=\rho^{\text{OPE}}(s,s',q^2)\theta(s-s_0)\theta(s'-s_0'), \tag{23}$$

where s_0 and s_0' are continuum thresholds in the initial and final mesonic channels, respectively. After these procedures, the following sum rules for the form factors are obtained:

$$
\begin{aligned}
K(q^2) &= \frac{8(m_b+m_u)}{f_B f_{D_2^*} m_{D_2^*}(m_B^2 q^2 - m_B^4 - 3m_B^2 m_{D_2^*}^2)} e^{\frac{m_B^2}{M^2}} e^{\frac{m_{D_2^*}^2}{M'^2}} \Bigg\{ \int_{(m_b+m_u)^2}^{s_0} ds \int_{(m_c+m_u)^2}^{s_0'} ds' \int_0^1 dx \int_0^{1-x} dy e^{\frac{-s}{M^2}} e^{\frac{-s'}{M'^2}} \\
&\times \Bigg[\frac{1}{256\pi^4 (x+y-1)^3} (2m_b(x+y-1)^3(4x^2-4y^2+3x-3y-3) + 3m_c(8x^5+6x^4(4y-3) \\
&- 6x(y-1)^2(3+2y+4y^2) - 2(y-1)^3(2+3y+4y^2) + 2x^3(1-18y+8y^2) + x^2(22-5y-16y^3))) \Bigg] \\
&\times \theta[L(s,s',q^2)] + e^{\frac{-m_b^2}{M^2}} e^{\frac{-m_c^2}{M'^2}} \Bigg[\frac{\langle \bar{u}u \rangle}{16} (m_b^2 + 2m_b m_c + m_c^2 - q^2) + \frac{m_0^2 \langle \bar{u}u \rangle}{64} \Bigg(2 + \frac{3m_b^2 + 2m_b m_c + 3m_c^2 - 3q^2}{M^2} \\
&- \frac{m_b^2 + 4m_b m_c + m_c^2 - q^2}{M'^2} - \frac{m_b^4 + 2m_b^3 m_c + m_b^2 m_c^2 - m_b^2 q^2}{M^4} - \frac{m_b^3 m_c + m_b^2 m_c^2 + 2m_b m_c^3 + m_c^4 - m_c^2 q^2}{M'^4} \\
&- \frac{m_b^4 + 4m_b m_c^3 + 2m_b^2 m_c^2 + m_c^4 - m_c^2 q^2 - m_b^2 q^2 + q^4}{M^2 M'^2} + \frac{m_b^5 m_c + m_b m_c^5 - m_b^2 m_c^2 q^2}{M^2 M'^4} \Bigg) \Bigg] \Bigg\}, \\
b_-(q^2) &= -\frac{12(m_b+m_u)}{f_B f_{D_2^*} m_B^2 m_{D_2^*}(m_B^4 + (m_{D_2^*}^2 - q^2)^2 - 2m_B^2(m_{D_2^*}^2 + q^2))} e^{\frac{m_B^2}{M^2}} e^{\frac{m_{D_2^*}^2}{M'^2}} \Bigg\{ \int_{(m_b+m_u)^2}^{s_0} ds \int_{(m_c+m_u)^2}^{s_0'} ds' \int_0^1 dx \int_0^{1-x} dy e^{\frac{-s}{M^2}} e^{\frac{-s'}{M'^2}} \\
&\times \Bigg[\frac{1}{128\pi^4 (x+y-1)^3} (m_b(x+y-1)^3(3-6x-2x^2+6y+2y^2) - 3m_c(6x^4(y-1) \\
&- 3x(y-1)^2(1+2y^2) - (y-1)^3(1+2y^2) + x^3(5-12y+4y^2) + x^2(1+4y-4y^3) + 2x^5)) \Bigg] \theta[L(s,s',q^2)] \\
&- e^{\frac{-m_B^2}{M^2}} e^{\frac{-m_{D_2^*}^2}{M'^2}} \frac{f_B f_{D_2^*} m_B^2 m_{D_2^*}(m_B^2 + 3m_{D_2^*}^2 + q^2)}{12(m_b+m_u)} K(q^2) \Bigg\}, \\
b_+(q^2) &= -\frac{12(m_b+m_u)}{f_B f_{D_2^*} m_B^2 m_{D_2^*}(m_B^4 + (m_{D_2^*}^2 - q^2)^2 - 2m_B^2(m_{D_2^*}^2 + q^2))} e^{\frac{m_B^2}{M^2}} e^{\frac{m_{D_2^*}^2}{M'^2}} \Bigg\{ \int_{(m_b+m_u)^2}^{s_0} ds \int_{(m_c+m_u)^2}^{s_0'} ds' \int_0^1 dx \int_0^{1-x} dy e^{\frac{-s}{M^2}} e^{\frac{-s'}{M'^2}} \\
&\times \Bigg[\frac{1}{128\pi^4 (x+y-1)^3} (m_b(x+y-1)^3(2x^2+2y^2+6x+6y+4xy-3) + 3m_c(2x^5 - 6x^4 + 10x^4 y \\
&+ (y-1)^3(1+2y^2) + x(y-1)^2(3-4y+10y^2) + x^2(20y^3 - 36y^2 + 20y - 5) \\
&+ x^3(7-24y+20y^2))) \Bigg] \theta[L(s,s',q^2)] - \frac{m_0^2 \langle \bar{u}u \rangle}{8} e^{\frac{-m_b^2}{M^2}} e^{\frac{-m_c^2}{M'^2}} - e^{\frac{-m_B^2}{M^2}} e^{\frac{-m_{D_2^*}^2}{M'^2}} \frac{f_B f_{D_2^*} m_B^2 m_{D_2^*}(m_{D_2^*}^2 - m_B^2 + q^2)}{12(m_b+m_u)} K(q^2) \Bigg\}, \\
h(q^2) &= \frac{8(m_b+m_u)}{f_B f_{D_2^*} m_B^2 m_{D_2^*}(m_{D_2^*}^2 - m_B^2 + q^2)} e^{\frac{m_B^2}{M^2}} e^{\frac{m_{D_2^*}^2}{M'^2}} e^{\frac{-m_b^2}{M^2}} e^{\frac{-m_c^2}{M'^2}} \Bigg\{ -\frac{\langle \bar{u}u \rangle}{16} + \frac{m_0^2 \langle \bar{u}u \rangle}{64} \Bigg[\frac{2}{M^2} + \frac{2}{M'^2} + \frac{m_b^2}{M^4} + \frac{m_c^2}{M'^4} + \frac{m_b^2 - m_c^2 + q^2}{M^2 M'^2} \Bigg] \Bigg\},
\end{aligned}
\tag{24}
$$

where

$$
\begin{aligned}
L(s,s',q^2) &= s'x - s'x^2 - m_c^2 x - m_b^2 y + sy + q^2 xy \\
&- sxy - s'xy - sy^2.
\end{aligned}
\tag{25}
$$

III. NUMERICAL RESULTS AND DISCUSSIONS

In this part, we numerically analyze the obtained sum rules for the form factors in the previous section and obtain their variations in terms of q^2. For this aim, we need some input parameters for which the values are given in Table I. Besides these input parameters, the sum rules for the form factors contain four auxiliary parameters, namely, the Borel mass parameters M^2 and M'^2 and continuum thresholds s_0 and s_0'. We shall find their working regions such that the form factors weakly depend on these parameters. The continuum thresholds are not completely arbitrary, but they are related to the energy of the first excited state in the initial and final mesonic channels. Our calculations show that, in the intervals $31\ \text{GeV}^2 \leq s_0 \leq 35\ \text{GeV}^2$ and $7\ \text{GeV}^2 \leq s_0' \leq 9\ \text{GeV}^2$, our results weakly depend on the continuum thresholds. The working regions for the Borel mass parameters are determined by requiring that not only the contributions of the higher states and continuum are sufficiently suppressed but also the contributions of the operators with higher dimensions are relatively small;

TABLE I. Input parameters used in calculations [10–14].

Parameters	Values
m_c	(1.275 ± 0.025) GeV
m_b	(4.65 ± 0.03) GeV
m_e	0.00051 GeV
m_μ	0.1056 GeV
m_τ	1.776 GeV
$m_{D_2^*(2460)}$	(2.4626 ± 0.0007) GeV
m_B	(5.27925 ± 0.00017) GeV
f_B	(210 ± 40) MeV
$f_{D_2^*(2460)}$	0.0317 ± 0.0092
G_F	1.17×10^{-5} GeV^{-2}
V_{cb}	$(41.2 \pm 1.1) \times 10^{-3}$
$\langle 0\|\bar{u}u(1\text{ GeV})\|0\rangle$	$-(0.24 \pm 0.01)^3$ GeV^3
$m_0^2(1\text{ GeV})$	(0.8 ± 0.2) GeV^2
τ_B	$(1641 \pm 8) \times 10^{-15}$ s

i.e., the series of sum rules for the form factors are convergent. As a result, we find the working regions $10\ \text{GeV}^2 \leq M^2 \leq 20\ \text{GeV}^2$ and $5\,\text{GeV}^2 \leq M'^2 \leq 15\,\text{GeV}^2$. To show how the form factors depend on the auxiliary parameters, as examples, we depict the variations of the form factors $K(q^2)$ and $b_+(q^2)$ at $q^2 = 0$ with respect to the variations of the related auxiliary parameters in their working regions in Figs. 1 and 2. From these figures, we see that the form factors weakly depend on the auxiliary parameters in their working regions.

Using the working regions for the continuum thresholds and Borel mass parameters as well as other input parameters, we proceed to find the behavior of the form factors in terms of q^2. Our calculations show that the form factors are truncated at $q^2 \simeq 5\ \text{GeV}^2$. To estimate the decay width of the $B \to D_2^*(2460)\ell\bar{\nu}$ transition, we have to obtain fit functions of the form factors in the whole physical region, $m_\ell^2 \leq q^2 \leq (m_B - m_{D_2^*})^2$. We find that the sum rules predictions for the form factors are well fitted to the following function:

$$f(q^2) = f_0 \exp\left[c_1 \frac{q^2}{m_{\text{fit}}^2} + c_2 \left(\frac{q^2}{m_{\text{fit}}^2}\right)^2\right], \tag{26}$$

where the values of the parameters f_0, c_1, c_2, and m_{fit}^2 are presented in Table II. In the following, we will recall this parametrization as *fit function 1*. To compare our results with the other parametrization, we also use the following fit functions to extrapolate the form factors to whole physical regions (see Refs. [15–18]):

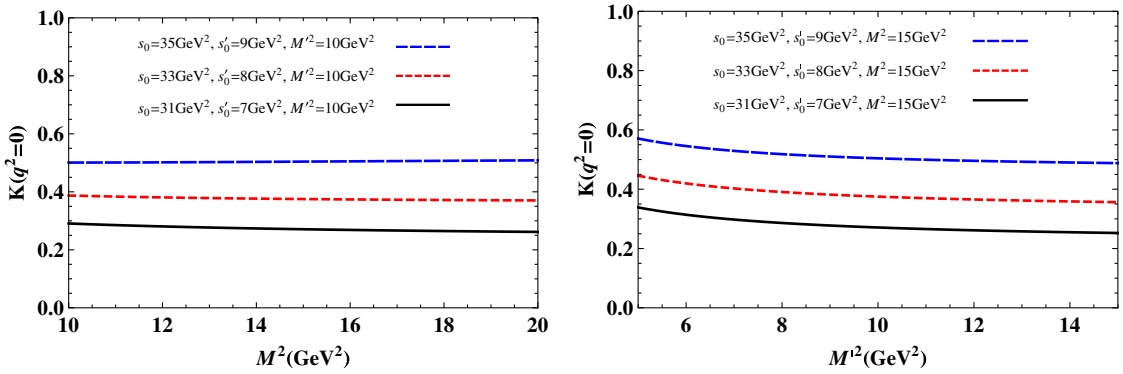

FIG. 1 (color online). Left: $\text{K}(q^2 = 0)$ as a function of the Borel mass M^2 at fixed values of the s_0, s_0', and M'^2. Right: $\text{K}(q^2 = 0)$ as a function of the Borel mass M'^2 at fixed values of the s_0, s_0', and M^2.

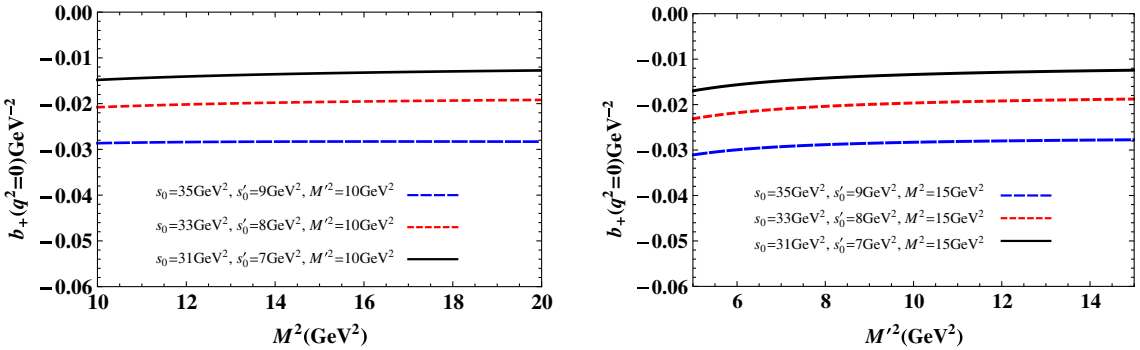

FIG. 2 (color online). Left: $b_+(q^2 = 0)$ as a function of the Borel mass M^2 at fixed values of the s_0, s_0', and M'^2. Right: $b_+(q^2 = 0)$ as a function of the Borel mass M'^2 at fixed values of the s_0, s_0', and M^2.

TABLE II. Parameters appearing in the fit function 1 of the form factors.

	f_0	c_1	c_2	$m^2_{\rm fit}$
$K(q^2)$	0.54 ± 0.14	0.70 ± 0.07	0.41 ± 0.02	27.88 ± 0.01
$b_-(q^2)$	0.007 ± 0.002 GeV^{-2}	0.14 ± 0.04	10.70 ± 0.82	27.88 ± 0.01
$b_+(q^2)$	-0.03 ± 0.01 GeV^{-2}	1.20 ± 0.15	22.52 ± 1.68	27.88 ± 0.01
$h(q^2)$	-0.010 ± 0.003 GeV^{-2}	1.19 ± 0.13	1.12 ± 0.08	27.88 ± 0.01

TABLE III. Parameters appearing in fit function 2 of the form factors.

	f_0	a	b
$K(q^2)$	0.54 ± 0.14	0.75 ± 0.03	-0.014 ± 0.006
$b_-(q^2)$	0.007 ± 0.002 GeV^{-2}	0.95 ± 0.04	-3.14 ± 1.34
$b_+(q^2)$	-0.03 ± 0.01 GeV^{-2}	1.41 ± 0.06	-4.63 ± 2.05
$h(q^2)$	-0.010 ± 0.003 GeV^{-2}	1.27 ± 0.05	0.058 ± 0.002

TABLE IV. Parameters appearing in fit function 3 of the form factors.

	f_0	A	B
$K(q^2)$	0.54 ± 0.14	-0.15 ± 0.06	0.31 ± 0.03
$b_-(q^2)$	0.007 ± 0.002 GeV^{-2}	-0.36 ± 0.16	-7.72 ± 0.86
$b_+(q^2)$	-0.03 ± 0.01 GeV^{-2}	1.89 ± 0.81	-2.39 ± 0.27
$h(q^2)$	-0.010 ± 0.003 GeV^{-2}	0.25 ± 0.10	-0.35 ± 0.04

(i) *fit function 2*:

$$f(q^2) = \frac{f_0}{1 - a(\frac{q^2}{m_B^2}) + b(\frac{q^2}{m_B^2})^2}, \tag{27}$$

(ii) *fit function 3*:

$$f(q^2) = \frac{f_0}{(1 - \frac{q^2}{m_B^2})[1 - A(\frac{q^2}{m_B^2}) + B(\frac{q^2}{m_B^2})^2]}, \tag{28}$$

where the parameters a, b, A, and B and the values of the corresponding form factors at $q^2 = 0$ are given in Tables III and IV, respectively.

The dependences of form factors on q^2 at different fixed values of auxiliary parameters are depicted in Figs. 3 and 4. These figures include the sum rules results (up to the truncated point) as well as the results obtained using the above-mentioned three different fit functions. From these figures, it is clear that, in the case of the form factors $K(q^2)$, $b_+(q^2)$ and $b_-(q^2)$, all three fit functions reproduce the sum

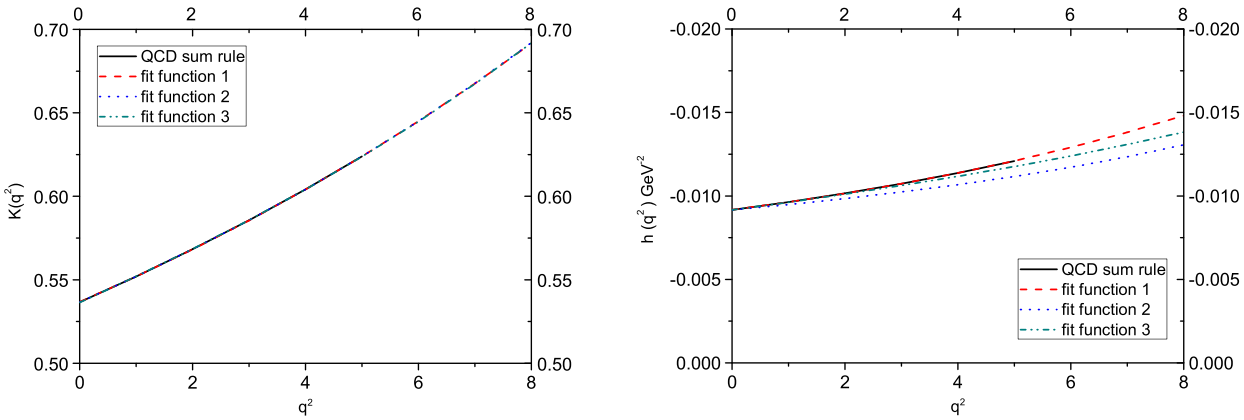

FIG. 3 (color online). Left: K(q^2) as a function of q^2 at $M^2 = 15$ GeV^2, $M'^2 = 10$ GeV^2, $s_0 = 35$ GeV^2, and $s'_0 = 9$ GeV^2. Right: h(q^2) as a function of q^2 at $M^2 = 15$ GeV^2, $M'^2 = 10$ GeV^2, $s_0 = 35$ GeV^2, and $s'_0 = 9$ GeV^2.

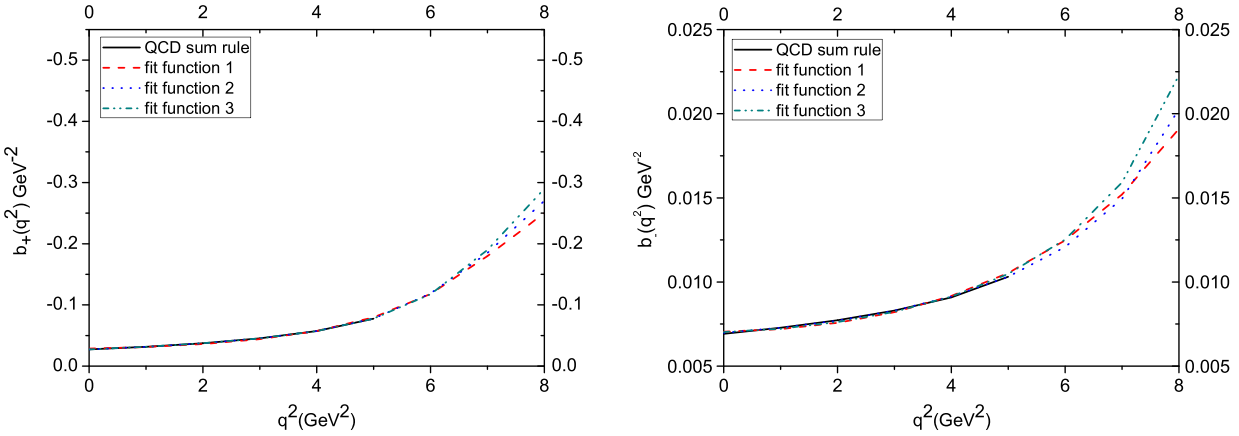

FIG. 4 (color online). Left: $b_+(q^2)$ as a function of q^2 at $M^2 = 15$ GeV^2, $M'^2 = 10$ GeV^2, $s_0 = 35$ GeV^2, and $s_0' = 9$ GeV^2. Right: $b_-(q^2)$ as a function of q^2 at $M^2 = 15$ GeV^2, $M'^2 = 10$ GeV^2, $s_0 = 35$ GeV^2, and $s_0' = 9$ GeV^2.

rules results up to the truncated point; however, we see small differences between the predictions of these fit functions at higher values of q^2 except for the form factor $K(q^2)$ that all fit functions give the same results. In the case of the form factor $h(q^2)$, parametrization 1 well fits to the sum rule result, but we see considerable differences of the prediction of this parametrization with those of fit functions 2 and 3, especially at higher values of q^2.

Now, we proceed to calculate the decay width and branching ratio of the process under consideration. The differential decay width for the $B \to D_2^*(2460)\ell\bar{\nu}$ transition is obtained as [19]

$$\frac{d\Gamma}{dq^2} = \frac{\lambda(m_B^2, m_{D_2^*}^2, q^2)}{4m_{D_2^*}^2}\left(\frac{q^2 - m_\ell^2}{q^2}\right)^2 \frac{\sqrt{\lambda(m_B^2, m_{D_2^*}^2, q^2)}G_F^2 V_{cb}^2}{384 m_B^3 \pi^3}\left\{\frac{1}{2q^2}\left[3m_\ell^2\lambda(m_B^2, m_{D_2^*}^2, q^2)[V_0(q^2)]^2 + (m_\ell^2 + 2q^2)\right.\right.$$
$$\times\left|\frac{1}{2m_{D_2^*}}\left[(m_B^2 - m_{D_2^*}^2 - q^2)(m_B - m_{D_2^*})V_1(q^2) - \frac{\lambda(m_B^2, m_{D_2^*}^2, q^2)}{m_B - m_{D_2^*}}V_2(q^2)\right]\right|^2\Bigg] + \frac{2}{3}(m_\ell^2 + 2q^2)\lambda(m_B^2, m_{D_2^*}^2, q^2)$$
$$\times\left[\left|\frac{A(q^2)}{m_B - m_{D_2^*}} - \frac{(m_B - m_{D_2^*})V_1(q^2)}{\sqrt{\lambda(m_B^2, m_{D_2^*}^2, q^2)}}\right|^2 + \left|\frac{A(q^2)}{m_B - m_{D_2^*}} + \frac{(m_B - m_{D_2^*})V_1(q^2)}{\sqrt{\lambda(m_B^2, m_{D_2^*}^2, q^2)}}\right|^2\right]\Bigg\}, \tag{29}$$

where

$$\begin{aligned} A(q^2) &= -(m_B - m_{D_2^*})h(q^2), \\ V_1(q^2) &= -\frac{K(q^2)}{m_B - m_{D_2^*}}, \\ V_2(q^2) &= (m_B - m_{D_2^*})b_+(q^2), \\ V_0(q^2) &= \frac{m_B - m_{D_2^*}}{2m_{D_2^*}}V_1(q^2) - \frac{m_B + m_{D_2^*}}{2m_{D_2^*}}V_2(q^2) - \frac{q^2}{2m_{D_2^*}}b_-(q^2), \\ \lambda(a, b, c) &= a^2 + b^2 + c^2 - 2ab - 2ac - 2bc. \end{aligned} \tag{30}$$

After performing integration over q^2 in Eq. (29) in the interval $m_\ell^2 \le q^2 \le (m_B - m_{D_2^*})^2$, we obtain the total decay widths and branching ratios for all leptons and three different fit functions presented in Table V. The errors in the results belong to the uncertainties in the determination of the working regions for the auxiliary parameters as well as errors in the other input parameters. From this table, it is clear that, for the e and μ channels, all fit functions give roughly the same results. In the case of τ, fit functions 2 and 3 have approximately the same predictions, but they

TABLE V. Numerical results for the decay widths and branching ratios at different lepton channels for different fit functions.

Fit function 1	Γ (GeV)	Br
$B \to D_2^*(2460)\tau\bar{\nu}_\tau$	$(6.52 \pm 2.20) \times 10^{-17}$	$(0.16 \pm 0.06) \times 10^{-3}$
$B \to D_2^*(2460)\mu\bar{\nu}_\mu$	$(4.04 \pm 1.18) \times 10^{-16}$	$(1.00 \pm 0.29) \times 10^{-3}$
$B \to D_2^*(2460)e\bar{\nu}_e$	$(4.05 \pm 1.19) \times 10^{-16}$	$(1.01 \pm 0.30) \times 10^{-3}$
Fit function 2	Γ (GeV)	Br
$B \to D_2^*(2460)\tau\bar{\nu}_\tau$	$(4.09 \pm 1.28) \times 10^{-17}$	$(0.10 \pm 0.03) \times 10^{-3}$
$B \to D_2^*(2460)\mu\bar{\nu}_\mu$	$(4.06 \pm 1.26) \times 10^{-16}$	$(1.01 \pm 0.32) \times 10^{-3}$
$B \to D_2^*(2460)e\bar{\nu}_e$	$(4.08 \pm 1.28) \times 10^{-16}$	$(1.02 \pm 0.32) \times 10^{-3}$
Fit function 3	Γ (GeV)	Br
$B \to D_2^*(2460)\tau\bar{\nu}_\tau$	$(4.80 \pm 1.60) \times 10^{-17}$	$(0.12 \pm 0.04) \times 10^{-3}$
$B \to D_2^*(2460)\mu\bar{\nu}_\mu$	$(4.18 \pm 1.32) \times 10^{-16}$	$(1.04 \pm 0.34) \times 10^{-3}$
$B \to D_2^*(2460)e\bar{\nu}_e$	$(4.20 \pm 1.32) \times 10^{-16}$	$(1.05 \pm 0.34) \times 10^{-3}$

give results roughly 38% smaller than those of fit function 1. As it is expected, the values for the branching ratios in the cases of e and μ are very close to each other for all fit functions. The orders of branching fractions show that this transition can be detected at the LHCb for all lepton channels. Note that there are experimental data on the products of branching fractions for the decay chain $\mathcal{B}(B \to D_2^*\ell\bar{\nu})\mathcal{B}(D_2^* \to D\pi)$ provided by the Belle [20] and *BABAR* [21,22] collaborations:

$$\mathcal{B}(B^+ \to \bar{D}_2^* \ell'^+ \bar{\nu}_{\ell'})\mathcal{B}(\bar{D}_2^* \to D\pi) = 2.2 \pm 0.3 \pm 0.4 \,\text{Belle},$$
$$\mathcal{B}(B^+ \to \bar{D}_2^* \ell'^+ \bar{\nu}_{\ell'})\mathcal{B}(\bar{D}_2^* \to D\pi) = 1.4 \pm 0.2 \pm 0.2 \,\textit{BABAR}, \tag{31}$$

where $l' = e$ or μ. Considering the recent experimental progress especially at the LHC, we hope we will have experimental data on the branching fraction of the semileptonic $B \to D_2^*(2460)\ell\bar{\nu}$ transition in the near future, the comparison of which to the results of the present work can give more information about the nature and internal structure of the $D_2^*(2460)$ tensor meson.

At the end of this section, we would like to calculate the ratio of the branching fraction in the case of τ to that of the e or μ. From our calculations, we obtain that

$$\mathcal{R} = \frac{B \to D_2^*(2460)\tau\bar{\nu}_\tau}{B \to D_2^*(2460)\ell'\bar{\nu}_{\ell'}} = \begin{cases} 0.16 \pm 0.04 & \text{fit function 1,} \\ 0.10 \pm 0.02 & \text{fit function 2,} \\ 0.11 \pm 0.02 & \text{fit function 3.} \end{cases} \tag{32}$$

As we previously mentioned, the standard model predictions in the B to pseudoscalar and vector charmed mesons deviate at the level of 3.4σ from the experimental data. Our result on $\mathcal{R}$ in the case of tensor charmed current can be checked in future experiments. Comparison of the experimental data with the result of this work will illustrate whether these anomalies in the pseudoscalar and vector channels exist also in the tensor channel or not.

[1] P. del Amo Sanchez *et al.* (*BABAR* Collaboration), Phys. Rev. D **82**, 111101 (2010).
[2] D. Becirevic, B. Blossier, A. Gerardin, A. Le Yaouanc, and F. Sanfilippo, Nucl. Phys. **B872**, 313 (2013).
[3] J. Segovia, C. Albertus, D. R. Entem, F. Fernandez, E. Hernandez, and M. A. Perez-Garcia, Phys. Rev. D **84**, 094029 (2011).
[4] F. De Fazio, Proc. Sci., HQL2012 (2012) 001.
[5] P. Colangelo, F. De Fazio, F. Giannuzzi, and S. Nicotri, Phys. Rev. D **86**, 054024 (2012).
[6] M. A. Shifman, A. I. Vainshtein, and V. I. Zakharov, Nucl. Phys. **B147**, 385 (1979).
[7] J. P. Lees *et al.* (*BABAR* Collaboration), Phys. Rev. Lett. **109**, 101802 (2012).
[8] S. Fajfer, J. F. Kamenik, and I. Nisandzic, Phys. Rev. D **85**, 094025 (2012).
[9] P. Biancofiore, P. Colangelo, and F. De Fazio, Phys. Rev. D **87**, 074010 (2013).
[10] J. Beringer *et al.* (Particle Data Group) Phys. Rev. D **86**, 010001 (2012).
[11] H. Sundu and K. Azizi, Eur. Phys. J. A **48**, 81 (2012).
[12] H. Na, C. J. Monahan, C. T. H. Davies, R. Horgan, G. P. Lepage, and J. Shigemitsu, Phys. Rev. D **86**, 034506 (2012).
[13] B. L. Ioffe, Prog. Part. Nucl. Phys. **56**, 232 (2006).

[14] H. G. Dosch, M. Jamin, and S. Narison, Phys. Lett. B **220**, 251 (1989); V. M. Belyaev and B. L. Ioffe, Sov. Phys. JETP **57**, 716 (1982).
[15] W. Wang, Phys. Rev. D **83**, 014008 (2011).
[16] R.-H. Li, C.-D. Lü, and W. Wang, Phys. Rev. D **83**, 034034 (2011).
[17] C.-D. Lü and W. Wang, Phys. Rev. D **85**, 034014 (2012).
[18] H.-Y. Cheng, C.-K. Chua, and C.-W. Hwang, Phys. Rev. D **69**, 074025 (2004).
[19] X.-X. Wang, W. Wang, and C.-D. Lü, Phys. Rev. D **79**, 114018 (2009).
[20] D. Liventsev *et al.* (Belle Collaboration), Phys. Rev. D **77**, 091503 (2008).
[21] B. Aubert *et al.* (*BABAR* Collaboration), Phys. Rev. Lett. **101**, 261802 (2008).
[22] B. Aubert *et al.* (*BABAR* Collaboration), Phys. Rev. Lett. **103**, 051803 (2009).